Dynamics of Blood Proteins Adsorption onto Poly (2-hydroxyethyl methacrylate)-Silica Nanocomposites: Correlation with Biocompatibility

A. K. Bajpai,[1] D. D. Mishra[2]

[1]*Bose Memorial Research Laboratory, Department of Chemistry, Government Autonomous Science College, Jabalpur, Madhya Pradesh 482 001, India*
[2]*Department of Chemistry, Shri Ram Institute of Technology, Marhotal, Jabalpur, Madhya Pradesh 482 001, India*

Received 7 June 2006; accepted 17 October 2006
DOI 10.1002/app.25654
Published online 24 September 2007 in Wiley InterScience (www.interscience.wiley.com).

ABSTRACT: A nanocomposite hybrid of poly(2-hydroxyethyl methacrylate) (PHEMA) and silica (PHEMA-Si) was prepared by sol–gel process and characterized by FTIR, environmental scanning electron microscopy (ESEM), and XRD techniques. The prepared hybrid was evaluated for its water sorption capacity and the adsorption of blood proteins such as bovine serum albumin (BSA) and fibrinogen (Fgn) was carried out on the hybrid surfaces. The dynamic nature of the adsorption process was investigated and related kinetic parameters were evaluated. The effect of factors like concentrations of protein solutions, pH, and ionic strength of the adsorption medium and chemical architecture of the hybrid were investigated on the adsorption process. The prepared hybrids were also examined for *in vitro* blood compatibility. © 2007 Wiley Periodicals, Inc. J Appl Polym Sci 107: 541–553, 2008

Key words: polymer; silica; composite; swelling; characterization; biocompatibility

INTRODUCTION

Interest in generating new materials for use as permanent implants has grown considerably in recent years.[1] Bioceramics consisting of organic polymers and inorganic oxide particles are widely used for biomedical applications.[2] In spite of a wide spectrum of application of polymer–inorganic particulate composites in diversified fields, several major problems in fabrication of such materials have been often encountered. For instance, providing a firm attachment between the polymer and inorganic phase, production of uniform size inorganic particles, homogeneous distribution of inorganic moieties over polymer phase, etc. have been such detrimental factors, which have to be addressed carefully for having a precise control over the properties and end use of the materials.[3]

Several synthetic routes have been adopted to design highly ordered polymer–inorganic oxide composites, which mainly includes free-radical polymerization of various monomers in the presence of colloidal solution,[4] blending of polymer solution and oxide particulate,[5] and precipitation of oxide within the polymer matrix.[6] However, a polymer–inorganic oxide composite with uniformly distributed particles of nanodimensions could only be made possible after the sol–gel process came into existence in mid 1980s when several silica–polymer hybrids were developed.[7] Till then, several excellent reviews have also appeared in the literature.[8]

The incorporation of polymeric components to sol–gel derived materials may constitute an important tool to either enhance mechanical properties[9] or provide more compatible media for encapsulation of biological molecules and medicines.[10] Thus, a big scope exists for designing and developing organic polymer–inorganic oxide composites with improved mechanical properties and enhanced biocompatibility, so as to deserve for biomedical applications such as biocatalysts, biosensors, immunodiagnostics, and drug-delivery systems.[11]

Undesirable blood material interactions are recognized problems in blood-contacting biomedical devices.[12] As soon as a material is placed within the body, it is covered in blood due to the incision made in the surrounding tissue. The blood–implant interaction starts a series of biological reactions (host response) that in the best case lead to successful integration of the implant, but in the worst case lead to a significant encapsulation.[13]

The first event that occurs in nanoseconds at the implant–tissue interface is that the water molecules

Correspondence to: A. K. Bajpai (akbmrl@yahoo.co.in).

and the salt ions reach the material surface.[14] The distribution of these molecules and ions is highly surface dependent and is very important for proteins and other molecules that arrive later.[15]

Protein adsorption on surfaces of biomaterials and medical implants is an essential aspect of the cascade of biological reactions taking place at the interface between a synthetic material and the biological environment.[16] Type, amount, and conformation of adsorbed proteins mediate subsequent adhesion, proliferation, and differentiation of cells and are believed to steer foreign body response and inflammatory processes.[17] Concerning the protein adsorption process, the fundamental electrostatic interactions between ceramic particles and proteins are only fragmentarily investigated and not well understood.[18]

Thus, realizing the potential significance of blood protein–material interaction in biomaterial science, the present study aims at studying adsorption of bovine serum albumin (BSA) and fibrinogen (Fgn) onto the surfaces of poly(2-hydroxyethyl methacrylate)-silica (PHEMA-Si) nanocomposites. The rational for selecting PHEMA as polymer component of the nanocomposite lies in its water imbibition property, thus letting: tissue in growth; high permeability to small molecules to have highly purified networks; soft consistency, which minimizes mechanical frictional irritation to surrounding tissues; low interfacial tension between the hydrogel and the aqueous solutions that can reduce proteins adsorption to the gel; and a large number of morphologies.[5] The proteins chosen for the present investigation are BSA and Fgn, which have been studied extensively due to their prominent role in coagulation.[6]

EXPERIMENTAL

Materials

2-Hydroxyethyl methacrylate (HEMA) was obtained from Sigma Aldrich, USA, and freed from the inhibitor following the method reported in our earlier communications.[19] The purity of HEMA was checked by a high-pressure liquid chromatograph (HPLC, Backmen System Cold 127) equipped with a UV detector, equipped with a 25 cm × 4.6 mm id separation columns (ODS C_{18}, 5 μm particle size). Tetramethoxysilane (TMOS) was purchased from Sigma Aldrich, USA, and used as received. Potassium persulphate (KPS) and sodium metabisulphite (MBS) employed as a redox couple were supplied by Qualigen Co. (Mumbai, India) and used without any pretreatment. Other chemicals were of AR grade and triple distilled water was used throughout the experiments.

Methods

Synthesis of hybrids

The method for the synthesis of hybrids was adopted from the literature.[20] The procedure is a two-step process and may be described briefly as follows: In the first step, PHEMA was synthesized by taking 32.9 m*M* HEMA, 71.6 m*M* ethylene glycol (cosolvent), and definite amount of water in a petri dish (diameter 4″, Corning). The whole mixture was homogenized by manual mixing and degassed by purging dry N_2 for 30 min. For initiating polymerization reaction, a redox couple comprising of degassed solutions of potassium persulphate (0.04*M*) and metabisulphite (0.3 m*M*) were added to the reaction mixture and polymerization was allowed to proceed for 24 h. The resulting polymer was allowed to swell in water, so that unreacted chemicals were leached out.

In the second step of the synthesis, a definite weight of gel (2.0 g) was dissolved into 30 mL of ethanol solution and to this solution was added 4 mL of TMOS and 2 mL of deionized water, which corresponds to water:TMOS molar ratio of about 4. After stirring the solution for 60 min, it was aged at 30°C for 4 days to allow gelation. The samples were then aged at 60°C for 40 h and finally dried for 48 h at 60°C and for 24 h at 100°C. In this way, a series of hybrids of varying compositions were prepared as summarized in Table I.

A gravimetric procedure was followed to the course of swelling. In brief, the dry hybrid buttons were allowed to swell in phosphate buffer saline (PBS, pH 7.4) and taken out after 7 days. Upon swelling, the gels again become spongy white. The white swollen gels were gently pressed in-between the filter papers to remove excess water and then weighed. The swelling ratio was calculated by the following equation:

$$\text{Swelling Ratio} = \frac{W_s}{W_d} \quad (1)$$

where W_s and W_d are the swollen and dry weights of the hybrids, respectively.

TABLE I
Water Sorption Capacity of PHEMA-Si Hybrids of Varying Chemical Compositions

PHEMA (g)	TMOS (m*M*)	Swelling ratio
1.0	27.1	2.62
2.0	27.1	3.64
3.0	27.1	4.20
4.0	27.1	4.34
2.0	6.78	1.78
2.0	13.5	2.20
2.0	20.3	2.88
2.0	27.1	3.64

Adsorption experiments

The adsorption of BSA and Fgn onto the buttons was performed by the batch process. For adsorption experiments, fresh protein solutions were made in 0.5*M* PBS at physiological pH 7.4. Before adsorption experiments, the hybrid buttons were equilibrated with PBS for 72 h. The adsorption was then carried out by gently shaking protein solutions of known concentration containing preweighed and fully swollen gels. By taking fully swollen gels, the possibility of absorption of protein solution within the gel becomes minimum. The shaking was performed so gently that no froth was produced; otherwise, it would have formed an air–water interface. After a definite time period, the gels were removed and the protein solution was assayed for the remaining concentration of BSA and Fgn by measuring absorbance at 278 and 280 nm, respectively, following a UV-spectrophotometric procedure (Systronics, Model No. 2201, India). The adsorbed amount of proteins (μg cm^{-2}) was calculated by the following mass-balance equation:

$$\text{Adsorbed Proteins} = \frac{(C_0 - C_e)\ V}{A} \tag{2}$$

where C_0 and C_e being the initial and equilibrium concentrations of BSA and Fgn proteins solutions (μg/mL), V is the volume of the protein solution, and A is the surface area of the swollen hybrids, i.e. the adsorbent determined by methylene blue adsorption method.[21]

For studying the kinetics of the adsorption process, the amount of adsorbed protein was determined at predetermined time intervals.

Blood compatibility tests

A biomaterial is a substance used in prostheses or in medical devices designed for contact with the living body for the intended method of application and for the intended period.[22] Synthetic polymers, the most diverse class of biomaterials, are widely used in both medical and pharmaceutical applications, and they contribute significantly to the quality and effectiveness of health care. These applications range from use in a variety of implants or other supporting materials (e.g., vascular grafts, artificial hearts, intraocular lenses, joints, mammary prostheses, and sutures to utilization in extracorporeal therapeutics and other supporting devices (e.g., hemodialysis, blood oxygenation, intravenous lines, and blood bags), controlled release systems (e.g., transdermal drug delivery patches and microspheres for targeted drug delivery devices for different routes of administration), and clinical diagnostic assays mainly as carriers and supporting materials.[23]

To be biocompatible, materials used in medical applications must meet certain criteria and regulatory requirements. The surfaces of biomaterials are believed to play an important role in determining biocompatibility. For materials that come in contact with blood, the formation of clot is the most undesirable but frequently occurring event that puts restriction on the clinical acceptance of material as a ''biomaterial.'' Therefore, certain test procedures have to be employed to judge the hemofriendly nature of the biomaterials.

Clot formation test. The antithrombogenic potential of the hybrid surfaces was judged by the blood-clot formation test as described elsewhere.[24] In brief, the hybrids were equilibrated with saline water (0.9% w/v NaCl) for 72 h in a constant temperature bath. To these swollen hybrids were added 0.5 mL of acid citrate dextrose (ACD) blood followed by the addition of 0.03 mL of $CaCl_2$ solution (4*M*) to start the thrombus formation. The reaction was stopped by adding 4.0 mL of deionized water, and the thrombus formed was separated by soaking in water for 10 min at room temperature and then fixed in 36% formaldehyde solution (2.0 mL) for another 10 min. The fixed clot was placed in water for 10 min, and after drying, its weight was recorded. The same procedure was repeated for the glass surface and sponges of varying compositions and the respective weights of thrombus formed were recorded by a highly sensitive balance (Denver, Germany).

Hemolysis assay. Hemolysis experiments were performed on the surfaces of the prepared sponges as described elsewhere.[25] In a typical experiment, a dry hybrid film (4 cm^2) was equilibrated in normal saline water (0.9% NaCl solution) for 24 h at 37°C and human ACD blood (0.25 mL) was added on the hybrid film. After 20 min, 2.0 mL of saline was added on the sponge to stop hemolysis, and the sample was incubated for 60 min at 37°C. Positive and negative controls were obtained by adding 0.25 mL of human ACD blood and saline solution, respectively, to 2.0 mL of bidistilled water. Incubated sample was centrifuged for 45 min, and the supernatant was taken and its absorbance was recorded on a spectrophotometer at 545 nm. The percent of hemolysis was calculated using the following relationship:

$$\%\ \text{Hemolysis} = \frac{A_{\text{test sample}} - A_{(-)\text{control}}}{A_{(+)\text{control}} - A_{(-)\text{control}}} \tag{3}$$

where a is the absorbance. The absorbance of positive and negative centers was found to be 1.764 and 0.048, respectively.

Characterization

FTIR Spectra

The IR spectra of dry PHEMA and hybrid were recorded on a Perkin–Elmer spectrophotometer (FTIR, Paragon 1000).

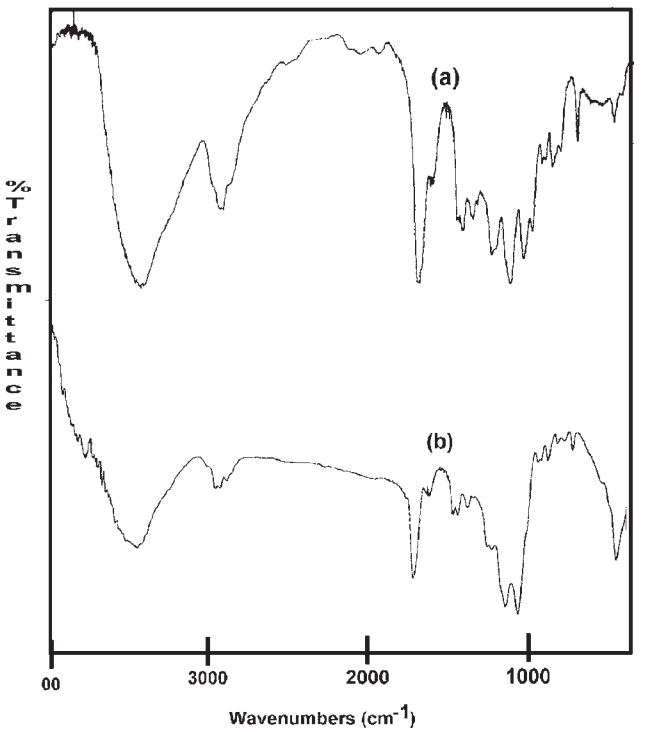

Figure 1 FTIR spectra of (a) PHEMA, and (b) PHEMA-Si hybrid.

Environmental Scanning Electron Micrograph (ESEM)

The surfaces of dry PHEMA and hybrids were examined by ESEM technique (STEREO SCAN, 430, Leica ESEM, USA).

RESULTS AND DISCUSSION

Characterization of Hybrids

FTIR spectral analysis

The IR spectra of PHEMA and PHEMA-Si hybrids are shown in Figure 1(a,b), respectively. The spectra (a) clearly marks the presence of OH group at 3439 and 1469 cm^{-1} (O—H stretching and bending, respectively),[26] CH_2 of methylene at 2946 cm^{-1} (C—H stretching), CO group at 1729 cm^{-1} (C=O stretching), and ester group at 1163 cm^{-1} (O—C—C stretching).

The spectra presented in Figure 1(b) shows the incorporation of silica into the PHEMA matrix. The peaks observed at 471 cm^{-1} due to Si—O—Si bending and at 909 cm^{-1} because of Si—O terminal nonbridging vibrations[27] confirm the presence of silica in the hybrid. A minor peak at 810 cm^{-1} is assigned to Si—O—Si bond vibration between two adjacent tetrahedral,[28] which also confirms the presence of silica in the hybrid.

The composite prepared in the present study is made of two phases: a pHEMA rich phase and a silica rich one, as confirmed by the observed bands as discussed earlier. As far as the interaction between polymer and silica phase is concerned, it is likely that covalent bonds might take place between organic and inorganic interfaces by heterocondensation reaction of HEMA hydroxyl groups and silanols. However, the presence of interfacial covalent bonds (Si—O—C) could not be detected by FTIR, which reveal that no extensive covalent interfacial bonds are formed in the hybrid.

Environmental scanning electron microscopy (ESEM)

Surface topography and roughness are important factors in determining the response of cells to a foreign material.[29] Surface with grooves can induce ''contact guidance'' whereby the direction of cell movement is affected by the morphology of the substrate.[30] Likewise, surface porosity has also been identified to affect the biocompatibility of polymeric biomaterials. Korbelar et al.[31] noticed an increase in biocompatibilty of PHEMA hydrogels with increasing pore sizes of the surfaces.

In the present study, the ESEM images of the PHEMA and PHEMA-Si hybrid are depicted in Figure 2(a,b), respectively. It is clear from the image (a) that PHEMA surface shows porous morphology while the later image clearly depicts how nanosize (40–400 nm) SiO_2 particles are distributed over the polymer (PHEMA) matrix. Thus, the PHEMA-Si hybrid may also be termed as nanocomposite.

Swelling of the Hybrid

The capacity of water absorption by a material is sometimes a prerequisite of the biomaterial and, therefore, has been investigated extensively.[32] The swelling ratio of hydrogels depends on their free volume, degree of chain flexibility, crosslink density, and hydrophilicity.[33] In the present study, also the swelling ratio of the prepared PHEMA-Si hybrids

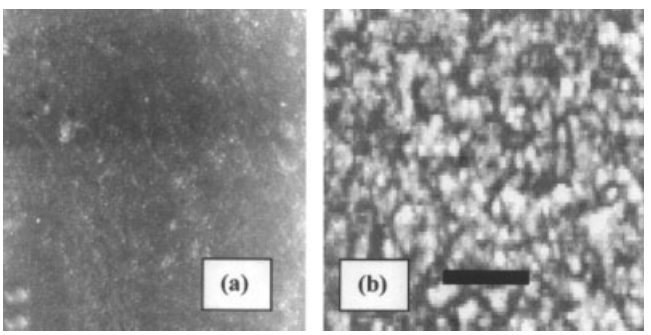

Figure 2 Environmental scanning electron microscopy (ESEM) images of the (a) PHEMA and (b) PHEMA-Si hybrid.

has been determined for various chemical compositions of the hybrids, and the data are summarized in Table I. It is clear from the results that the swelling ratio is significantly affected by the chemical composition of the hybrids as discussed below.

When the concentration of PHEMA is increased in the feed mixture of the hybrid in the range 1.0–4.0 g, the water sorption capacity constantly increases. The observed increase may be attributed to the fact that HEMA is a hydrophilic monomer, and therefore, its increasing content in the hybrid results in a more hydrophilic polymer matrix, which obviously brings about an increase in the water imbibition capacity.

The effect of variation in the silica content of the hybrids on their swelling ratio has also been studied by increasing the concentration of TMSO in the range 6.78–27.1 m*M*. The results summarized in Table I clearly reveal that the swelling ratio increases with increasing SiO_2 content in the hybrid. The increase observed may be attributed to the presence of hydrated silica in the hybrid. Thus, an increase in swelling ratio is expected.[34]

Protein–surface interactions

In protein–surface interactions, the governing forces are determined both by the physical state of the material and protein surface and the intimate solution environment. Factors including bound ions, surface charge, surface roughness, surface elemental composition, and surface energetics, etc. all have to be considered in defining the role of the solid–solution interface.[35]

Most surfaces acquire some charge when exposed to ionic solutions. In such cases, the electrostatic interaction, which is long-ranged, will dominate protein adsorption kinetics. Because of the long ranged nature of the electrostatic interactions protein may be guided into a unique orientation when approaching the oppositely charged surface. Although a charged protein is expected to prefer adsorption onto an oppositely charged surface, the osmotic pressure of counter ions, charged group desolvation, and burying of the charges into a low dielectric medium may, in fact, counteract protein adsorption. If considered alone, electrostatic interactions may not fully account to attachment of proteins to the charged interface. In the case of like charges between the surface and a protein, an energy barrier to adsorption may develop. If the overall charge of protein is zero, i.e. at isoelectric point, the electrostatic interaction between protein and surface may still exist, because the charge distribution on the protein surface is not uniform.

Proteins are large amphipathic compounds possessing multiple functional groups on their hydrophilic and hydrophobic domains. In aqueous solution, the hydrophobic portion is shielded from water, whereas the hydrophilic part is exposed to the adsorbing surface. In a similar way, the polymer matrix may also contain hydrophilic and hydrophobic segments (or groups), which could interact with the adsorbing protein molecules. Thus, the interaction forces between protein molecules and polymer particles can be classified as hydrophobic interactions, ionic (or electrostatic bonding), hydrogen bonding, and van der Waals interactions.

In the present study, the hydroxyl and carboxyl groups of each repeat unit of PHEMA and oxide of silica impart hydrophilicity to the hybrid matrix, whereas the α-methyl groups and backbone of PHEMA provide hydrophobicity and mechanical strength to the hybrid. Thus, a combined effect of hydrophilic and hydrophobic interactive forces between the hybrid and protein molecules may lead to their adsorption.

Modeling of protein adsorption isotherms

Many protein adsorption modeling approaches have been tried and several have been refined to be considerable successful.[36] Colloidal-scale models represent the protein as a particle and can accurately predict protein adsorption kinetics and isotherms. These colloidal scale models include explicit Brownian dynamics type models,[37] random sequential adsorption models,[38,39] scaled particle theory,[40] slab models,[41] and molecular theoretical approaches.[42] Most of these approaches treat the electrostatistics and van der Waals interactions between the protein and the surface, and thus can capture dependencies on surface charge, protein dipole moment, protein size, or solution ionic strength.

Although the correlation between the adsorbed protein and bulk concentration of protein solution has been dealt with many adsorption isotherm equations,[43] however, the Langmuir equation has been the first choice of researchers because of its computational simplicity and ease of applicability to various adsorption data. In the present study, the following two empirical equations have been used:

The Freundlich adsorption isotherm

$$C_s = k\, C_b^{1/m} \tag{4}$$

contains two parameters. The constant k is a measure of the capacity of the adsorption and exponent $(1/m)$ is a measure of the intensity of adsorption.

Another equation used is the linearized Langmuir equation:

$$\frac{C_b}{C_s} = \frac{C_b}{C_L} + \frac{1}{C_L} K^{-1} \tag{5}$$

where C_b and C_s are bulk and surface protein concentrations, C_L is monotonically reached limiting sur-

face concentration, and K is a parameter, which describes the strength of interaction between the protein and the surface.

Generally speaking, proteins adsorb on any surface with only a few exceptions. The fractional coverage is, therefore, strongly dependent on the bulk concentration of proteins.

The effect of initial concentration of BSA and fibrinogen solutions on the adsorbed amount of proteins has been investigated by varying their initial concentrations in the range 500–4500 and 55–850 μg/mL, respectively. The results clearly indicate that the adsorbed amount gradually increases with increasing concentration of protein solutions and ultimately attains a limiting value, which is indicative of the formation of a monolayer on the hybrid surfaces. The observed increase may be attributed to the fact that with increasing bulk concentration of protein solution, a greater number of protein molecules arrive at the sponge–water interface and get adsorbed over the sponge surfaces.

A more quantitative information about the protein–surface interaction may be obtained by constructing an adsorption isotherm, which is normally obtained by plotting the adsorbed amount of proteins against the residual concentration of the protein solution. The adsorption isotherms obtained in the present case are shown in Figure 3, which indicate a typical Langmuir type of curve, which is characterized by an initial rising portion followed by a plateau portion. Similar type of isotherms have been frequently reported in the literature.[44] The adsorption isotherm constants for both BSA and Fgn have been summarized in Table II.

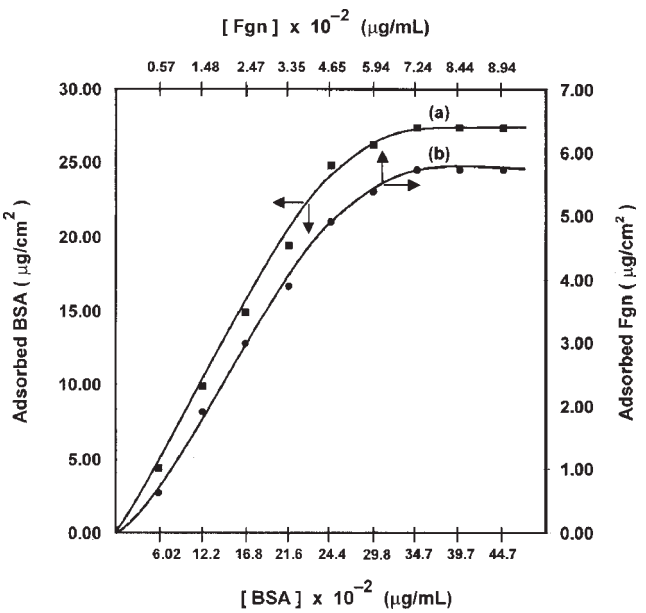

Figure 3 Adsorption isotherms of (a) BSA and (b) Fgn for adsorption on to the PHEMA-Si surfaces of definite composition [PHEMA] = 2.0 g, [TMOS] = 27.1 m*M*, [Ionic strength] = 0.001*M*, KNO_3, Temp. = (37 ± 0.2)°C, pH = 7.4.

TABLE II
Data Showing the Various Kinetic Constants for Adsorption of Proteins Onto the PHEMA-Si Hybrids

Parameters	Bovine serum albumin (BSA)	Fibrinogen (Fgn)
Freundlich constants		
k	2.71	4.04
$(1/m)$	0.75	0.86
Langmuir constant $K \times 10^4$	2.38	12.5
Rate constant for adsorption $(k_1) \times 10^6$	1.3	3.33
Rate constant for desorption $(k_2) \times 10^3$	2.3	2.0
Association constant $(k_A) \times 10^4$	5.6	16.6

Analysis of kinetic constants

In Freundlich equation, the constants k and $1/m$ represent predicted quantity of sorption for 1 g of the adsorbent at unit equilibrium concentration and measure of nature and strength of adsorption forces, respectively. The data summarized in Table II clearly indicate that both the above-mentioned parameters are higher for fibrinogen than BSA, which suggest for greater affinity of fibrinogen to adsorption than BSA.

Similarly, Langmuir constant k for fibrinogen is nearly more than five times greater than that for BSA. Likewise, greater rate constant of adsorption (k_1) for fibrinogen than that for BSA also indicates a faster adsorption of the former than that of the latter. This is further supported by the observation that equilibrium adsorption reach earlier in the case of fibrinogen than in the case of BSA as evident from adsorbed protein versus time plots. A greater affinity of fibrinogen for adsorbent is also evident from the higher value of association constant (k_A) for fibrinogen than for BSA.

Effect of pH and ionic strength

The pH of an adsorption medium has a significant influence on the amount of adsorbed protein. The effect is much more observable, particularly in those systems which involve ionic type of adsorbate and adsorbent surfaces. In the present case, since due to silica the hybrid is ionic in nature; the effect of pH on adsorption is jointly determined by both the proteins molecule and silanol groups whose net charges vary with the pH of the solution. The effect of pH

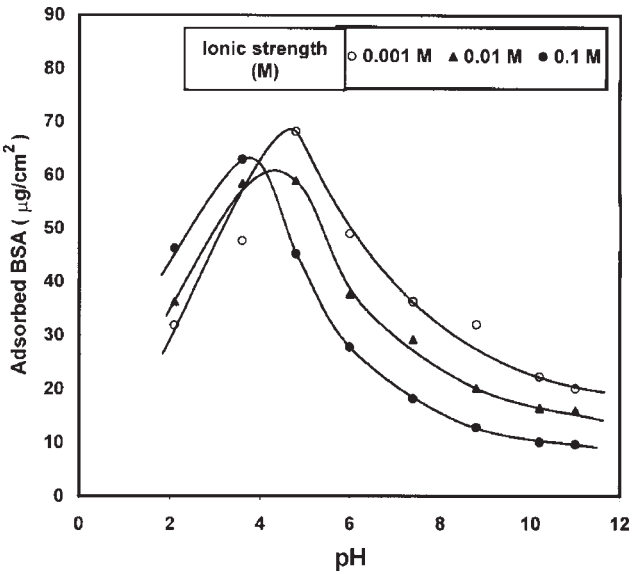

Figure 4 Adsorption isotherms for BSA at various pH and ionic strength of the protein solution adsorbing on to the PHEMA-Si hybrid surfaces of definite composition [PHEMA] = 2.0 g, [TMOS] = 27.1 m*M*, [Ionic strength] = 0.001*M*, KNO_3, Temp. = (37 ± 0.2)°C, pH = 7.4.

on the adsorption of BSA and fibrinogen has been investigated by varying pH of the protein solution in the range 2.1–11.0. The results are depicted in Figures 4 and 5, respectively, which clearly imply that a maximum adsorption is noticed at pH 4.8, which is near to the isoelectric points of BSA (4.8) and fibrinogen (5.1), respectively. The optimum adsorption of proteins at their isoelectric points is a common phenomenon in protein–surface interaction.[45]

The observed optimum adsorption of proteins at the isoelectric point may be because of the reason that at isoelectric point the lateral interactions among BSA and Fgn molecules are minimized and the protein acquires a compact conformation. Thus, a greater number of protein molecules can adsorb on the given surface area of the hybrid.

Another reason for the optimum adsorption near pH 4.8 may be that at this pH the protein molecules possess equal number of positive and negative charges, and the composite surface bears a negative charge (due to SiO^-). Thus, the protein molecules with positive functional head adsorb onto the negatively charged adsorbent surface and show an optimum adsorption. However, as the pH is increased beyond 4.8, the protein molecules acquire net negative charge and thus a continuous fall in adsorption is noticed with further increase in pH of the protein solution. The observed fall is attributed to the existing repulsion forces operative between the protein molecules and hybrid surface.

An interesting feature revealed by Figures 4 and 5 is that the adsorption isotherms constructed for various ionic strengths respond differently to pH of the adsorption medium. It is clearly shown in the figure that as the ionic strength increases the maxima present in the isotherm becomes more and more pronounced. The observed results may be attributed to the reason that at lower ionic strength, the density of fibrinogen molecules at the hybrid solutions interface will be low and a less number of protein molecules are operative at the active sites for adsorption. Thus, the lateral interactions among the molecules are not indifferent and significant at, below and above the isoelectric point of the protein. As a consequence of this, the adsorbed proteins also do not vary appreciably, thus giving an isotherm of less pronounced maxima. On the other hand, at higher ionic strength, greater number of proteins molecules causes a greater degree of lateral interactions and, therefore, result in a pronounced maxima.

Another important observation is that the shape of the adsorption isotherm is appreciably affected by the ionic strength of the medium as shown in Figures 4 and 5. It is implied by the results shown that in the acidic range the amount of adsorbed proteins increase with increasing ionic strength of the medium. The observed increase may be due to the reason that with increasing ionic strength, the electrostatic repulsions decrease in the interior of protein molecules, which leads protein molecules to form more compact structures. Moreover, lateral repulsions between the adsorbed protein molecules also decrease with increasing ionic strength and, thus, a greater number of molecules can adsorb onto the given surface area.

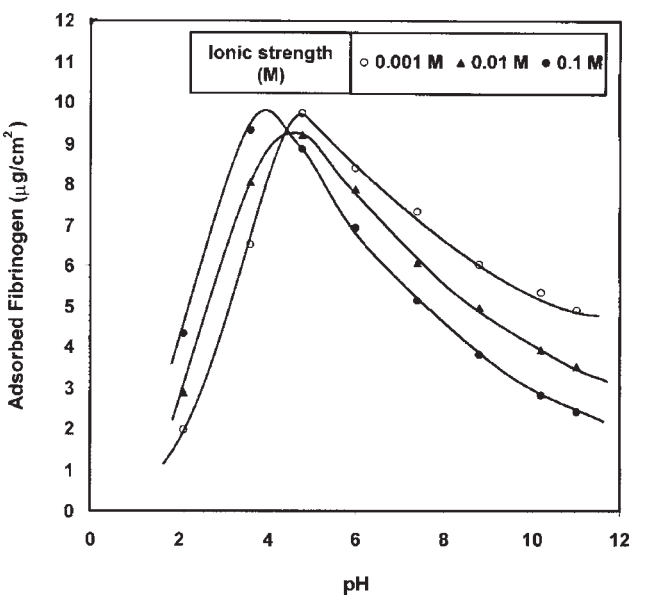

Figure 5 Adsorption isotherms at various pH and ionic strength of the protein solution for Fgn adsorbing on to the PHEMA-Si hybrid surfaces of definite composition [PHEMA] = 2.0 g, [TMOS] = 27.1 m*M*, [Ionic strength] = 0.001*M*, KNO_3, Temp. = (37 ± 0.2)°C.

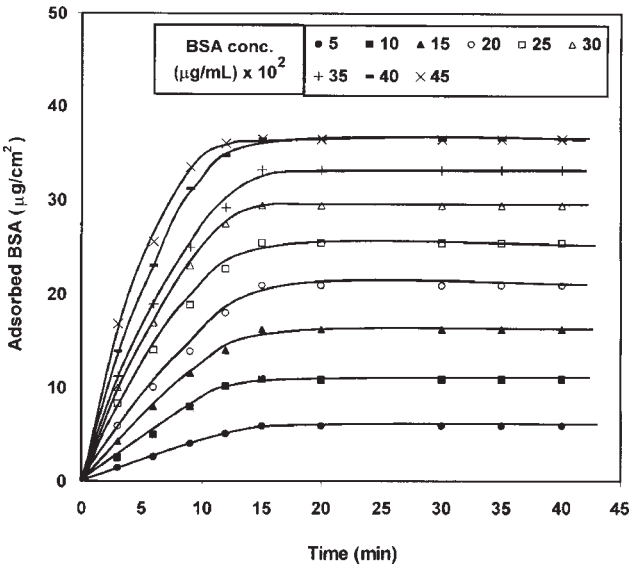

Figure 6 Plots showing the progress of the adsorption process for BSA adsorbing from protein solutions of varying concentrations on to the PHEMA-Si hybrid surfaces of definite compositions [PHEMA] = 2.0 g, [TMOS] = 27.1 m*M*, [Ionic strength] = 0.001*M*, KNO_3, Temp. = (37 ± 0.2)°C, pH = 7.4.

It is also revealed by the figure that the maxima at which the adsorption of proteins becomes optimum is slightly shifted towards acidic pH range with increasing ionic strength. This shifting of the maxima has been observed earlier also.[46]

Dynamics of proteins adsorption

The adsorption of proteins from its aqueous solution onto a solid surface is normally considered to occur in three steps[47]: (i) diffusion of protein molecules from bulk to the interface, (ii) attachment of protein molecules to active sites on the surface, and (iii) reconformation of the structure of the protein molecule after adsorption. Of these steps, the third step plays a significant role not only in controlling the adsorption kinetics of proteins, but also in modification of the surface properties of the substrate.

The dynamics of the adsorption process was followed by determining the amounts of adsorbed BSA and Fgn at various time intervals, as shown in Figures 6 and 7, respectively. It is clear from the figure that the rate of adsorption is almost constant up to 10 min, and then it gradually slows down attaining a limiting value after 20 min. The kinetic profile of the adsorption process may be explained by the fact that the adsorption of functionalized large chains (such as proteins) is a two regime process.[48] At the initial stages, the hybrid surface is bare, and the kinetics of adsorption is governed by the diffusion of the chains from the bulk solution to the surface. All the BSA and fibrinogen molecules arriving at the interface are considered to be immediately adsorbed. The mass transport can be interpreted as a Fickian diffusion. The diffusion coefficient can be determined by the following equation:

$$q = \frac{2}{\pi} C_o \sqrt{Dt} \tag{6}$$

From the slope of the curve drawn between q (adsorbed protein) and $\sqrt{t}$, for BSA and Fgn solutions of varying concentrations the diffusion constants can be calculated as summarized in Table III. It is revealed from Table III that, with an increasing concentration of protein solutions, the diffusion constants constantly decrease. The observed decrease may be attributed to the fact that as the bulk concentration of protein solution increases the BSA and Fgn molecules approaching at the substrate–solution interface have to go across a thicker protein layer near the interface and, therefore, diffuse slowly. Similar type of lower diffusion constants at higher protein concentration have also been reported.[48] This is expected also from the Ficks law of diffusion since the concentration gradient at the hybrid–solution surface increases with increase in the initial concentration of BSA and fibrinogen solutions.

In the later stage of adsorption process, a barrier of adsorbed molecules exists, and the molecules arriving from solution have to diffuse across this barrier. This penetration is slow, and a theoretical treatment given by Ligorue and Leibler predicts an exponential time dependence for the later stages.[49]

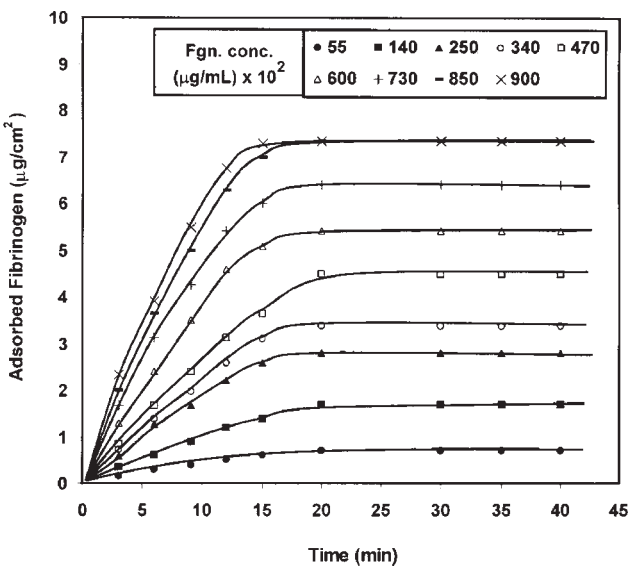

Figure 7 Plots showing the progress of the adsorption process for Fgn adsorbing from protein solutions of varying concentrations on to the PHEMA-Si hybrid surfaces of definite compositions [PHEMA] = 2.0 g, [TMOS] = 27.1 m*M*, [Ionic strength] = 0.001*M*, KNO_3, Temp. = (37 ± 0.2)°C, pH = 7.4.

TABLE III
Variation of Diffusion Constant (D) and Penetration Constant ($1/\tau$) with Bulk Concentration of Protein Solutions

Bovine serum albumin (BSA)			Fibrinogen (Fgn)		
Bulk concentration (μg/mL)	$1/\tau$ (10^3 s^{-1})	D (10^7 cm^2/s^{-1})	Bulk concentration (μg/mL)	$1/\tau$ (10^3 s^{-1})	D (10^7 cm^2/s^{-1})
5	2.60	2.22	55	2.08	3.26
10	3.67	1.79	140	2.31	2.54
15	4.62	1.68	250	2.77	2.21
20	5.09	1.54	340	2.97	1.73
25	5.20	1.51	470	3.20	1.23
30	5.55	1.41	600	3.47	1.15
35	6.25	1.38	730	3.78	1.12
40	7.50	1.24	850	4.16	0.98

$$q(t) = q_{eq}[1 - \exp(-t/\tau)] \quad (7)$$

where q_{eq} is the adsorbed amount at equilibrium and $1/\tau$ is the penetration rate constant (τ is also known as relaxation time). This equation suggests that the second process has an exponential nature, and the penetration rate may be obtained from the slope of the plot of $[\ln(q_e - q)]$ as a function of time. From the slopes of the straight lines (not shown), the penetration rate constants for varying bulk concentration of BSA and Fgn have been calculated and summarized in Table III.

The results clearly reveal that the penetration constant ($1/\tau$) increases with increasing bulk and surface concentration of proteins. The observed increase is quite obvious as at higher bulk and surface concentration, the protein molecules diffuse more slowly and thus require greater time for penetration to get adsorbed onto the hybrid surfaces.

Kinetic model for adsorption

The kinetic model described by Tanaka and coworkers[50] may be successfully employed to investigate the dynamic nature of the adsorption process. In brief, the protein adsorption on polymer surface (hybrid) may be described by the following eq. (8)

$$[\text{Polymer}] + [\text{Protein}] \underset{k_2}{\overset{k_1}{\rightleftharpoons}} [\text{Polymer}-\text{Protein}]^* \underset{k_4}{\overset{k_3}{\rightleftharpoons}} [\text{Polymer}-\text{Protein}] \quad (8)$$

In the above equation [Polymer–Protein]* represents the metastable complex composed of the polymer surface and the protein. In the early stage of protein adsorption, it is assumed that the reaction on the polymer surface can be simply described by the following eq. (9), which reveals that the extent of adsorption depends on the amount of the complex.

$$[\text{Polymer}] + [\text{Protein}] \underset{k_2}{\overset{k_1}{\rightleftharpoons}} [\text{Polymer}-\text{Protein}] \quad (9)$$

On the basis of the above equation, the production rate of metastable complex can be given by the following equation:

$$\frac{d}{dt}[\text{Polymer} - \text{Protein}]^* = k_1[\text{Polymer}][\text{Protein}] - k_2[\text{Polymer}-\text{Protein}]^* \quad (10)$$

The amount of the complex formed at time t is given by eq. (11):

$$[\text{Polymer} - \text{Protein}]^*_t = [\text{Polymer}-\text{Protein}]^*_\infty \times (1 - e^{(-1/\tau)t}) \quad (11)$$

where [Polymer–Protein] is the concentration of the complex at theoretical time ∞, τ is the relaxation time of the adsorption, and the reciprocal of τ is defined by the following eq. (12).

$$\tau^{-1} = k_1[\text{Protein}]_0 + k_2 \quad (12)$$

where $[\text{Protein}]_0$ is the initial concentration of the proteins. The complete derivation of the above equation may be seen in the Ref. 50. The eq. (12) clearly indicates that from the slope and intercept of the plot drawn between τ^{-1} and $[\text{Protein}]_0$, the values of k_1, k_2, and k_1/k_2 ($= k_A$) may be calculated. In the present study, the kinetic parameters calculated for the adsorption of BSA and Fgn have been summarized in Table II.

Effect of Fgn concentration on adsorption kinetics

The adsorption of fibrinogen is well-known to exhibit different adsorption behavior at low and high protein flux conditions,[51] thus, indicating a history dependence on the ultimate surface coverage.[52] Initially, it was suggested that the fibrinogen can exist

in two distinct conformations on surfaces, resulting in two experimentally observable populations: a larger irreversibly adsorbed layer on a smaller reversibly adsorbed layer.[53] However, recent studies have revealed that fibrinogen can exist in many possible orientations and/or conformations depending on the adsorption history and the surface chemistry of the substrate.[51] It was also shown that fibrinogen adsorbs nonspecifically to both hydrophobic and hydrophilic surfaces, resulting in a random mixture of end-on and side-on oriented molecules initially. Following attachment to the surface fibrinogen begins to increase its foot print (i.e. the number of segment–surface contacts) in a manner that is consistent with denaturation (unfolding) on hydrophobic surfaces and reorientation (rolling over) on hydrophilic surfaces. Thus, reversibly and irreversible bound populations may consist of many different protein footprint sizes, not only as two distinct conformations.

Thus, realizing the impact of protein flux on the adsorption dynamics of fibrinogen onto the hybrid surfaces, the influence of bulk concentration of protein solution has been investigated on the dynamic nature of the adsorption process by monitoring the progress of the adsorption process at different bulk concentration varying in the range 950–1200 μg/mL. The results shown in Figure 8 are quite unusual and the adsorption profiles appear unlike any of the other protein. The results clearly reveal that at low solution concentrations the adsorption reach at a plateau value, whereas at higher concentration range (i.e. from 950 to 1200 μg/mL) the adsorbed amount of fibrinogen attains an optimum value and, thereafter, decreases with increasing time. Similar type of results have also been published elsewhere.[54] The results can be interpreted as below:

The diffusion-controlled nature of the adsorption process, as discussed previously, reveals that each collision between fibrinogen molecule and the sponge surface results in an adsorption event. The initial increase in adsorption with increasing bulk concentration of protein solution may obviously be due to the fact that greater number of fibrinogen molecules interact with the surface and adsorb reversibly with end-on orientation. It is important to note that due to end-on orientation of adsorbed fibrinogen molecules footprint size becomes small, and consequently, less contact is established between the sponge surface and the adsorbed segments of fibrinogen molecule, which eventually results in a reversible adsorption. It is well-known that fibrinogen (MW: 340,000–400,000 Da) is an exceptionally elongated molecule with an axial ratio (major axis:minor axis) of about 18:1. It contains about 10% charged residues and is negatively charged at pH 7.4 (IP about 5.1).

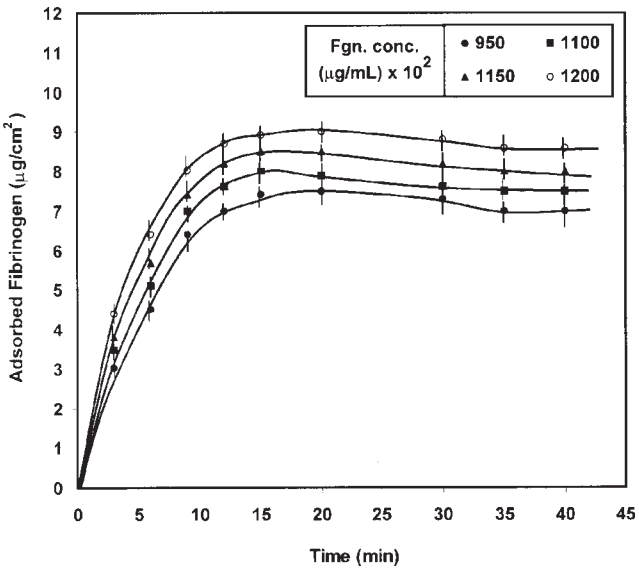

Figure 8 Plots showing the progress of the adsorption process for Fgn adsorbing from protein solutions of higher bulk concentrations on to the PHEMA-Si hybrid of definite compositions [PHEMA] = 2.0 g, [TMOS] = 27.1 m*M*, [Ionic strength] = 0.001*M*, KNO_3, Temp. = (37 ± 0.2)°C, pH = 7.4.

Now, at higher concentration (>850 μg/mL) of the protein solution, the adsorbed fibrinogen molecules are forced to undergo conformational transition from end-on to side-on adsorption, so that the footprint size of the adsorbed protein molecules increases. The increased contact with the sponge surface results in a firm binding to the surface, thus, changing the adsorption from reversible to irreversible one. It is interesting to realize here that due to side-on orientation of adsorbed fibrinogen molecules, the hybrid surfaces are shielded from the other approaching molecules and, therefore, the adsorbed amount of fibrinogen decreases.

Effect of solution and biological fluids

The influence of solute and media on the adsorption of fibrinogen was examined by performing adsorption experiments in the presence of solutes such as potassium iodide (15% w/v), urea, and D-glucose (5% w/v), and in physiological fluids, such as saline water (0.9% NaCl) and artificial urine. The adsorption results are presented in Table IV, which clearly reveal that in all the cases, a fall in adsorbed amount is noticed. The observed results can be explained by the fact that the salt ions present in the adsorption media also compete with the adsorbing protein molecules and thus partially exhaust available active sites on the sponge surfaces. This obviously results in a fall in the adsorption of fibrinogen.

TABLE IV
Adsorption of Proteins onto PHEMA-Si Hybrid[a] in Various Simulated Biological Fluids

Physiological fluids	Adsorbed protein ($\mu g/cm^2$) BSA	Fgn
Phosphate buffer saline (pH 7.4)	36.5	7.34
KI (15% w/v)	30.4	6.68
Urea (5% w/v)	28.6	6.02
D-glucose (5% w/v)	34.2	5.92
Saline water (0.9% w/v)	23.8	4.86
Synthetic urine[b]	20.2	5.02

[a] [PHEMA] = 2.0 g, [TMOS] = 27.1 m*M*, Temp. = (37 ± 0.2)°C.
[b] NaCl (0.8% w/v), $MgSO_4$ (0.10% w/v), Urea (21% w/v), $CaCl_2$ (0.06% w/v).

TABLE V
Effect of Chemical Composition of the Hybrid on the Adsorbed Amount of Proteins

PHEMA (g)	TMOS (m*M*)	Adsorbed protein BSA ($\mu g/cm^2$)	Fgn ($\mu g/cm^2$)
1.0	27.1	42.6	9.60
2.0	27.1	36.5	7.34
3.0	27.1	28.4	6.86
4.0	27.1	19.8	5.44
2.0	6.78	22.2	4.81
2.0	13.5	28.8	5.88
2.0	20.3	31.6	6.24
2.0	27.1	36.5	7.34

Effect of hybrid composition on protein adsorption

It is a well-recognized fact that the composition and organization of the adsorbed protein layer can be varied by numerous factors relating to the substrate, such as hydrophobicity, sorbed water content, microphase separation, and surface chemical functionality. As far as the chemistry of surface is concerned, the hydrophilic and hydrophobic balance of constituent chains in polymer surfaces has been found to play a key role in influencing protein adsorption and subsequent platelet adhesion to polymer surfaces.[55] In the present investigation also, the effect of composition of the hybrid on the adsorbed BSA and Fgn has been studied and the observed results are summarized in Table V.

The results clearly reveal that as the concentration of PHEMA increases in the range 1.0–4.0 g, the proteins adsorption constantly decrease. The fall noticed in the amount of adsorbed proteins may be explained by the fact that as the PHEMA content in the hybrid increases the surface area and pore volume also decrease significantly as reported elsewhere.[20] Thus, the amount of adsorbed proteins will also decrease.

Similarly, increasing TMOS concentration in the feed mixture of the hybrid in the range 6.78–27.1 m*M* results in a hybrid with greater SiO_2 content in the hybrid, which, consequently, results in an increase in the surface area as well as pore volume of the porous hybrid. This obviously facilitates protein diffusion into the hybrid and, therefore, brings about an increase in the amounts of adsorbed proteins.

Blood clot formation and hemolysis

The basic factors that govern compatibility of biomaterials are not completely understood. In particular, the design of biocompatible synthetic surfaces that are able to control the interaction between a living system and an implanted material remains a major theme for biomedical applications in medicine.

A great deal of experimental work has been confined to fabricate a biomaterial that lasts long without failure when put in contact with a stream of flowing blood under *in vivo* conditions. The fundamental approach behind the above task has been to minimize the extent of thrombus formation on blood-contacting devices, thus to synthesize a nonthrombogenic polymer. The rationale for the development of these nonthrombogenic polymers is to prevent activation of the thrombogenic pathway by tailoring polymer surfaces to minimize blood interaction. An alternative route to achieve a nonthrombogenic polymeric implants has been to design a material with very low affinity for protein adsorption since, as mentioned earlier also, a thin layer of protein is formed at the blood–material interface within a few seconds after flowing blood contacts a foreign surface. Subsequent cellular events, such as adhesion and aggregation of platelets that initiate clot formation, are most likely mediated by this protein layer, instead of by the material surface itself. As different surfaces show different affinity for protein adsorption, the clot formation may also be a function of the chemical architecture of the materials and their surface as well.

The clot formation and percent hemolysis data are presented in Table VI, which clearly reveal that both the *in vitro* blood compatibility parameters vary with the chemical composition of the PHEMA-Si hybrid. It is clearly shown in the Table that when the concentration of PHEMA increases in the hybrid there occurs a significant fall in both the clot formation and percent hemolysis, which could be attributed to the enhanced hydrophilic nature of the composite. As discussed earlier, the PHEMA rich hybrid also tends to adsorb less protein, which also indicates for enhanced blood compatibility.

On the other hand, increasing silica content in the hybrid results in an increased clot formation and percent hemolysis as clear from the data summar-

TABLE VI
Blood Compatibility Parameters of the PHEMA-Si Hybrids of Varying Chemical Compositions

PHEMA (g)	TMOS (m*M*)	Weight of blood clot (mg)	Hemolysis (%)
1.0	27.1	8.04	14.6
2.0	27.1	3.84	8.2
3.0	27.1	2.94	7.8
4.0	27.1	2.04	6.40
2.0	6.78	1.28	2.6
2.0	13.5	2.12	4.2
2.0	20.3	2.44	6.6
2.0	27.1	3.84	8.2
Glass surface		42.4	31.4

ized in the Table. The reason for a decreased blood compatibility of the silica rich hybrid may be attributed to the greater amounts of proteins adsorption which obviously facilitate more clot formation and percent hemolysis as well.

CONCLUSIONS

Inclusion of silica into PHEMA matrix by sol–gel process results in a hybrid in which covalent bonds might take place between at organic–inorganic interfaces by heterocondensation reactions of HEMA hydroxyl groups and silanols. The presence of both PHEMA and silica in the hybrid is confirmed by FTIR analysis. A close examination of the morphology of the hybrid surface by ESEM technique reveal the nanocomposite nature of the hybrid in which nanosize silica particles are distributed over the PHEMA matrix. The crystalline nature of the hybrid is also confirmed by the XRD analysis.

The PHEMA-Si hybrid shows hydrophilic nature and increasing content of both PHEMA and silica in the hybrid results in an enhanced swelling ratio.

The prepared hybrid surface shows less affinity for adsorption of BSA and Fgn; however, relatively more adsorption of BSA is noticed in comparison to Fgn. The adsorption of both the proteins is found to follow Langmuirian nature and show a plateau in their isotherms at the surface concentrations of 36.5 and 7.34 μg/mL for BSA and Fgn, respectively.

The adsorption of proteins shows a greater dependence on both pH and ionic strength of the adsorption medium, thus, exhibiting maxima in their adsorption at pH near to the isoelectric points of the proteins. The increasing ionic strength tends to shift the maxima to a little lower pH value.

Both the BSA and Fgn show an increasing adsorption with increasing bulk concentration of the two proteins solutions; however, at much higher concentration of Fgn solution, a decrease in adsorption is noticed.

The adsorption of both BSA and Fgn proteins depend on the chemical composition of the hybrid. The adsorption decreases with increasing PHEMA content while larger silica content tends to enhance the amounts of adsorbed proteins.

The hybrid surfaces show a fair level of blood compatibility especially at higher and lower content of PHEMA and silica, respectively.

REFERENCES

1. Salernitano, E.; Migliaresf, C. J Appl Biomater Biomech 2003, 1, 3.
2. Ahmad, H.; Miah, M. A. J.; Rahman, M. M. Colloid Polym Sci 2003, 281, 988.
3. Wang, Y.-X.; Robertson, J. L.; Spillman, W. B.; Claus, R. O. Pharmaceut Res 2004, 21, 1362.
4. Barthet, C.; Hickey, A. J.; Cairns, D. B.; Annes, S. P. Adv Mater 1999, 11, 408.
5. Constantini, A.; Luciani, G.; Annunziata, G.; Silvestri, B.; Branda, F. J Mater Sci, Mater Med 2006, 17, 319.
6. Martins, M. C. L.; Wang, D.; Ji, J.; Feng, L.; Barbosa, M. A. J Biomater Sci Polym Edn 2003, 14, 439.
7. Pope, E. J. A.; Asami, M.; Mackenzie, J. D. J Mater Res 1989, 4, 1018.
8. Chujo, Y.; Tamaki, R. MRS Bull 2001, 26, 389.
9. Kamitakahara, M.; Kawashita, M.; Miyata, N. J Sol–Gel Sci Tech 2001, 21, 75.
10. Avnir, D.; Braun, S.; Lev, O.; Ottolenghi, M. Chem Mater 1994, 6, 1605.
11. Ratner, B. D.; Bryant, S. J Annu Rev Biomed Eng 2004, 6, 41.
12. Castner, D. G.; Ratner, B. D. Surf Sci 2002, 1–3, 28.
13. Anderson, J. M. Annu Rev Mater Res 2001, 31, 81.
14. Rosengren, A.; Pavlovic, E.; Oscarsson, S.; Krajewski, A.; Ravaglioli, A.; Piancastelli, A. Biomaterials 2002, 4, 1237.
15. Collier, T. O.; Anderson, J. M. J Biomed Mater Res 2002, 60, 487.
16. Rezwan, K.; Meier, L. P.; Gauckler, L. J. Biomaterials 2005, 26, 4351.
17. Bucciantini, E. G.; Chiti, F.; Baroni, F.; Formigli, L.; Zurdo, J.; Taddei, N. R. G.; Dobson, C. M.; Stefani, M. Nature 2002, 416, 507.
18. Lee, W. K.; Ko, J.-S.; Kim, H.-M. J Colloid Interface Sci 2002, 246, 70.
19. Bajpai, A. K. Polym Int 2004, 53, 261.
20. Costa, R. O. R.; Pereira, M. M.; Lameiras, F. S.; Vasconcelos, W. L. J Mater Sci, Mater Med 2005, 16, 927.
21. Santamarina, J. C.; Klein, K. A.; Wang, Y. H.; Prencke, E. Can Geotech 2002, 39, 233.
22. Park, J. B.; Bronzino, J. D. Biomaterials: Principles and Applications; CRC Press: Boca Raton, FL, 2003.
23. Hoffman, A. S. Adv Drug Deliv Rev 2002, 43, 3.
24. Imai, Y.; Nose, Y. J Biomed Mater Res 1972, 6, 165.
25. Singh, D. K.; Ray, A. K. J Appl Polym Sci 1994, 53, 1115.
26. Klee, D.; Hocker, H. Adv Polym Sci 2000, 149, 1.
27. Huang, Y.; Jiang, Z.; Schwieger, W. Chem Mater 1999, 11, 1210.
28. Ohtsuki, C.; Kokubo, T.; Yamamuro, T. J Non Cryst Solids 1992, 143, 84.
29. Puleo, D. A.; Nanci, A. Biomaterials 1999, 20, 2311.
30. Brunnette, D. M. Int J Oral Maxillofac Implants 1988, 3, 231.
31. Korbelar, P.; Vacik, J.; Dylevsky, I. J Biomed Mater Res 1988, 22, 751.
32. Kim, S. J.; Shin, S. R.; Lee, Y. M.; Kim, S. I. J Appl Polym Sci 2003, 87, 2011.
33. Bosch, P.; Monte, F. D.; Mateo, J. L.; Levy, D. J. J Polym Sci, Part A: Polym Chem 1996, 34, 3289.

34. Branda, F.; Constantini, A.; Luciani, G.; Ambrosio, L. Biomed J Mater Res 2001, 57, 79.
35. Israelachvili, J. Intermolecular and Surface Forces, 2nd ed.; Academic Press: London, 1992.
36. Morra, M. J Biomater Sci Polym Edn 2000, 11, 547.
37. Oberholzer, M. R.; Lenhoff, A. M. Langmuir 1999, 15, 3905.
38. Feder, J. J Theor Biol 1980, 87, 237.
39. Bartelt, M. C.; Privman, V. Int J Mod Phys B 1991, 5, 2883.
40. Brusatori, M. A.; van Tassel, P. R. J Colloid Interface Sci 1999, 219, 333.
41. Stahlberg, J.; Jonsson, B. Anal Chem 1996, 68, 1536.
42. Fang, F.; Szleiter, I. Biophys J 2001, 80, 2568.
43. Roth, C. M.; Lenhoff, A. M. Surf Sci Ser 1998, 75, 89.
44. Kayirhan, N.; Denizli, A.; Hasirci, N. J Appl Polym Sci 2001, 81, 1322.
45. Norde, W. Adv Colloid Interface Sci 1986, 25, 267.
46. Bajpai, A. K.; Mishra, D. D. J Mater Sci Mater Med 2004, 15, 583.
47. Dijit, J. C.; Cohen Stuart, M. A.; Hoffman, J. F.; Flecr, G. J Colloids Surf 1990, 51, 141.
48. Siqueria, D. F.; Breiner, U.; Stadler, R.; Stamm, M. Langmuir 1996, 12, 972.
49. Ligoure, C.; Leibler, L. J Phys (Paris) 1990, 51, 1313.
50. Tanaka, M.; Mochizaki, A.; Shiroya, T.; Motomura, T.; Shimurak, K.; Onishi, M.; Okahata, Y. Colloids Surf A 2002, 203, 195.
51. Wertz, C. F.; Santore, M. M. Langmuir 2001, 17, 3006.
52. Wertz, C. F.; Santore, M. M. Langmuir 1999, 15, 8884.
53. MacRitichie, F. J Colloid Interface Sci 1972, 38, 484.
54. Wertz, C. F.; Santore, M. M. Langmuir 2002, 18, 706.
55. Wahlgren, M.; Arnebrant, J. Trends Biotechnol 1991, 6, 201.